



# The Receptor–CheW Binding Interface in Bacterial Chemotaxis

Anh Vu, Xiqing Wang, Hongjun Zhou and Frederick W. Dahlquist\*

Department of Chemistry and Biochemistry, University of California Santa Barbara, Santa Barbara, CA 93106-9510, USA

Received 11 September 2011;  
received in revised form  
19 November 2011;  
accepted 27 November 2011  
Available online  
6 December 2011

Edited by M. F. Summers

## Keywords:

chemotaxis;  
CheW;  
receptor;  
MCP;  
negative cooperativity

The basic structural unit of the signaling complex in bacterial chemotaxis consists of the chemotaxis kinase CheA, the coupling protein CheW, and chemoreceptors. These complexes play an important role in regulating the kinase activity of CheA and in turn controlling the rotational bias of the flagellar motor. Although individual three-dimensional structures of CheA, CheW, and chemoreceptors have been determined, the interaction between chemoreceptor and CheW is still unclear. We used nuclear magnetic resonance to characterize the interaction modes of chemoreceptor and CheW from *Thermotoga maritima*. We find that chemoreceptor binding surface is located near the highly conserved tip region of the N-terminal helix of the receptor, whereas the binding interface of CheW is placed between the  $\beta$ -strand 8 of domain 1 and the  $\beta$ -strands 1 and 3 of domain 2. The receptor–CheW complex shares a similar binding interface to that found in the “trimer-of-dimers” oligomer interface seen in the crystal structure of cytoplasmic domains of chemoreceptors from *Escherichia coli*. Based on the association constants inferred from fast exchange chemical shifts associated with receptor–CheW titrations, we estimate that CheW binds about four times tighter to its first binding site of the receptor dimer than to its second binding site. This apparent anticooperativity in binding may reflect the close proximity of the two CheW binding surfaces near the receptor tip or further, complicating the events at this highly conserved region of the receptor. This work describes the first direct observation of the interaction between chemoreceptor and CheW.

© 2011 Elsevier Ltd. All rights reserved.

## Introduction

The bacterial chemotaxis signaling system is one of the most well understood in biology. During chemotaxis, motile bacteria modulate their swimming behavior to direct their movement toward optimal environments by tracking temporal changes in chemical concentrations with high sensitivity and over a wide range of concentrations.

\*Corresponding author. E-mail address: [dahlquist@chem.ucsb.edu](mailto:dahlquist@chem.ucsb.edu).

Abbreviations used: 3D, three-dimensional; TROSY, transverse relaxation optimized spectroscopy; HSQC, heteronuclear single quantum coherence; HMQC, heteronuclear multiple quantum coherence.

The basic structural unit of the signaling complex in chemotaxis consists of chemotaxis kinase (CheA), coupling protein (CheW), and transmembrane receptors called methyl-accepting proteins, or MCPs (methyl-accepting chemotaxis proteins). In the most completely understood receptor systems, reversible methylation and attractant ligand binding are opposing events that the signaling complexes use to regulate the autophosphorylation activity of CheA. This opposed modulation of kinase activity enables the cell to make comparison of the past and current environments and to control the activity of CheA in response to this comparison.<sup>1</sup> Once autophosphorylated, CheA transfers its phosphoryl group to the small soluble protein CheY; then, CheY~P diffuses to the flagellar motor, where it binds, and enhances the switching of the flagellar

motor from the counterclockwise to clockwise rotational state.

The best-understood chemotaxis receptors consist of a periplasmic domain that interacts with the appropriate target ligand, a transmembrane region followed by a HAMP domain<sup>1</sup> that acts as a signal conversion module, and then by a large cytoplasmic domain. The cytoplasmic portion of the receptor interacts with CheA and CheW. The cytoplasmic region of the receptor consists of a long helical region that folds back on itself to form a long two-stranded antiparallel coiled coil. Each monomer of the receptor is assembled into dimers to form a four-stranded coiled coil that seems to be the basic structural unit of the cytoplasmic region of all chemotaxis receptors.<sup>2</sup> To date, crystal structures of the receptor cytoplasmic domains from *Escherichia coli* and *Thermotoga maritima* have been published. The cytoplasmic domains of all these receptors share the four-stranded coiled-coil structure and have a region of remarkable sequence similarity at the tip region where the individual chains fold back on themselves.<sup>2</sup> In Fig. 1, the crystal

structure of a portion of the soluble receptor TM0014 is shown in a cartoon representation of the backbone (left) where the individual polypeptide chains can be seen. Residues 90–206 (TM0014<sub>90–206</sub>) are shown in a space-filling representation (right) and include the conserved tip region. This receptor region has been implicated by genetic and biochemical means as the site of interaction with CheA and CheW.

CheW is a coupling protein that plays an important role in the formation of the receptor–signaling complex. It contains two  $\beta$  sheet domains. Each domain consists of a five-stranded  $\beta$ -barrel that forms an internal hydrophobic core for protein–protein interaction. Its structure is quite similar to that of CheA P5 domain, and it is known that they interact with each other.<sup>3,4</sup>

There have been several studies on the interaction of the chemoreceptor complexes with other chemotactic proteins.<sup>5–9</sup> Although the crystal structure of CheA containing the CheW and receptor coupling domains (P4P5) in *T. maritima* has been solved,<sup>4</sup> the interaction between the chemoreceptors and CheW is still unclear. The three-dimensional (3D) structures of CheW and TM0014 have been solved by nuclear magnetic resonance (NMR) and X-ray crystallography, respectively.<sup>3,4</sup> The chemotaxis proteins from *T. maritima* are well behaved at millimolar concentration and are stable at up to 90 °C. This makes them well suited for structural analysis by solution NMR methods. Here, we report the identification of a binding interface between chemoreceptor TM0014 and CheW from *T. maritima* using NMR methods.

## Results

TM0014 is a soluble receptor without the transmembrane regions.<sup>10</sup> Each monomer in the four-helix bundle dimer has 213 residues. The extended shape of this protein makes its effective size significantly larger than a globular protein of comparable molecular weight. Its rotational diffusion properties are unfavorable for detailed NMR studies of the backbone of the dimer. To facilitate high-resolution NMR study of the receptor backbone, we constructed a shorter fragment of the receptor, TM0014<sub>90–206</sub>, that contains the helix bundle tip region of the full-length receptor and a 5 His tag and an additional tyrosine residue (used to determine protein concentration) at its N-terminus. As expected, both the tyrosine mutant and TM0014<sub>90–206</sub> showed the same chemical shift perturbation in the <sup>1</sup>H–<sup>15</sup>N transverse relaxation optimized spectroscopy (TROSY)–heteronuclear single quantum coherence (HSQC) spectra upon addition of CheW, confirming that the tyrosine mutant does not perturb the CheW–receptor interaction.

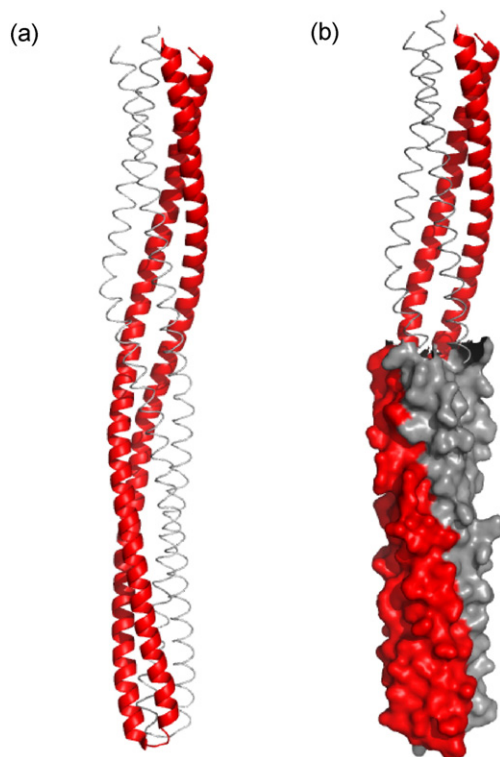


**Fig. 1.** Ribbon and worm diagrams of the structure of TM0014 (a) showing the two monomer chains (red and gray). (b) A representation of the short construct TM0014<sub>90–206</sub> in a space-filling view (red and gray) using the coordinates of TM0014. The ribbon and worm representations show those residues deleted in the shortened construct.

## Sequential assignment of the receptor fragment

The backbone amide assignments of the receptor fragment TM0014<sub>90–206</sub> were completed using TROSY-based HNCACB, HNCA, HNCOCACB, and HNCOCACB experiments (see [Experimental Procedures](#)). We used U-[<sup>2</sup>H,<sup>15</sup>N,<sup>13</sup>C]TM0014<sub>90–206</sub> for the backbone assignment. [Figure 2a](#) showed the assigned <sup>1</sup>H–<sup>15</sup>N TROSY–HSQC spectrum of TM0014<sub>90–206</sub>. The backbone amide resonances of TM0014<sub>90–206</sub> were well dispersed with mostly sharp resonances at 40 °C. A total of six residues were unassigned because we were not able to detect their backbone amide resonances in the 3D spectra. These residues were Lys90, Ser91, Gly92, Thr93, and Asn94 at the N-terminus and Glu149 located right at the center of the tip region. The missing resonances of Lys90, Ser91, Gly92, Thr93, Asn94, and Glu149 could be due to dynamic effects of conformational heterogeneity and/or solvent-exchange effects. [Figure 2b](#) shows a plot of chemical shift index<sup>11</sup> as a function of

residue number. As can be seen in the figure, the secondary structure of the fragment is largely helical with a distinct break at residues 146–151 corresponding to the position where the polypeptide chain folds back on itself to form the tip of the receptor.

## The receptor binding interface of CheW

We performed chemical shift perturbation mapping with CheW labeled with {[U-<sup>2</sup>H,<sup>12</sup>C], Ile,<sub>γ1</sub>-[<sup>13</sup>CH<sub>3</sub>], Leu,Val-[<sup>13</sup>CH<sub>3</sub>]}<sup>12</sup> but otherwise deuterated by titrating it with protonated and deuterated TM0014<sub>90–206</sub> and TM0014. The CheW interface residues are identified by comparing the spectra collected with a protonated partner and a deuterated partner.<sup>13</sup> [Figure 3a](#) shows the Ile, Leu, and Val methyl side-chain spectrum of {[U-<sup>2</sup>H,<sup>12</sup>C], Ile,<sub>γ1</sub>-[<sup>13</sup>CH<sub>3</sub>], Leu,Val-[<sup>13</sup>CH<sub>3</sub>]}CheW in the presence of an excess of deuterated TM0014<sub>90–206</sub>. Comparing the isoleucine, valine, and leucine methyl group spectra of CheW alone (black) and CheW in the

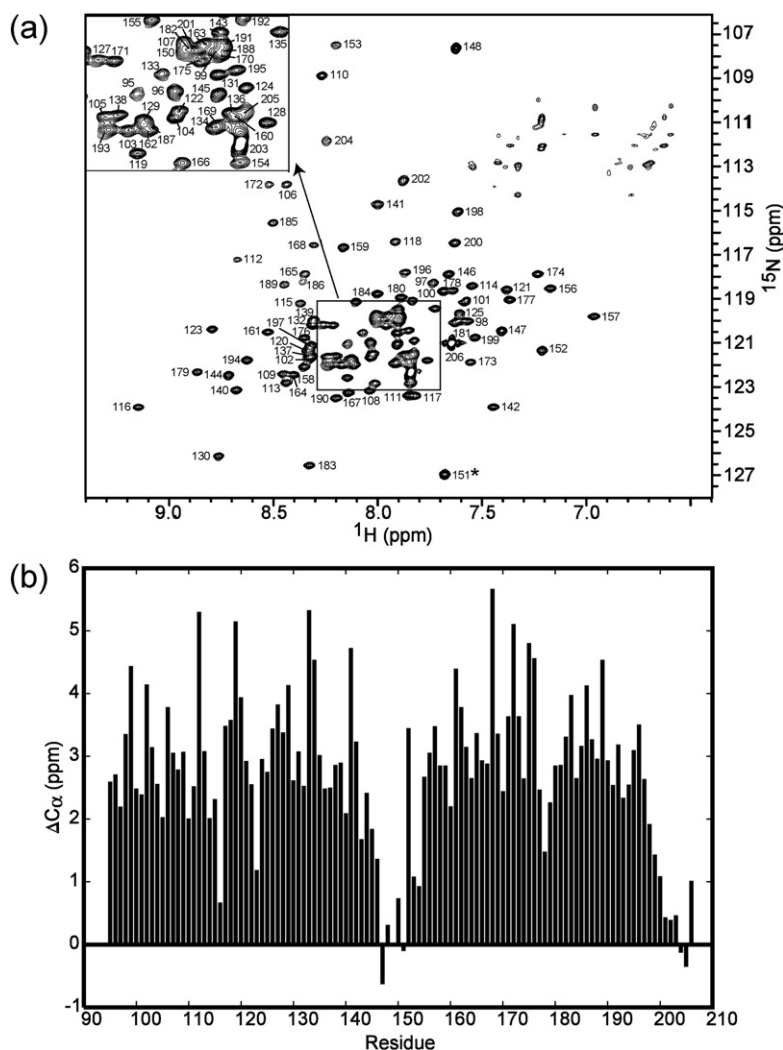


**Fig. 2.** The assigned <sup>1</sup>H–<sup>15</sup>N TROSY–HSQC spectrum and the secondary structure analysis of TM0014<sub>90–206</sub>. (a) <sup>1</sup>H–<sup>15</sup>N correlation map of <sup>15</sup>N-labeled TM0014<sub>90–206</sub> from *T. maritima* collected at 40 °C and pH 7.4. The assignment of backbone amides is indicated with sequence numbers. Asterisks indicate aliasing of the peaks from outside the spectral window along <sup>15</sup>N dimension. The central region enclosed by the square is expanded and represented as a small section in the upper left corner of the spectrum. (b) The differences between the observed C<sup>α</sup> chemical shifts of residues 90–206 and their respective random-coil chemical shifts were plotted as a function of residue number. Continuous stretches of positive ΔC<sub>α</sub> are indicative of helices, while the small stretches with both positive and negative ΔC<sub>α</sub> values at residues 146–151 are suggestive of loops.

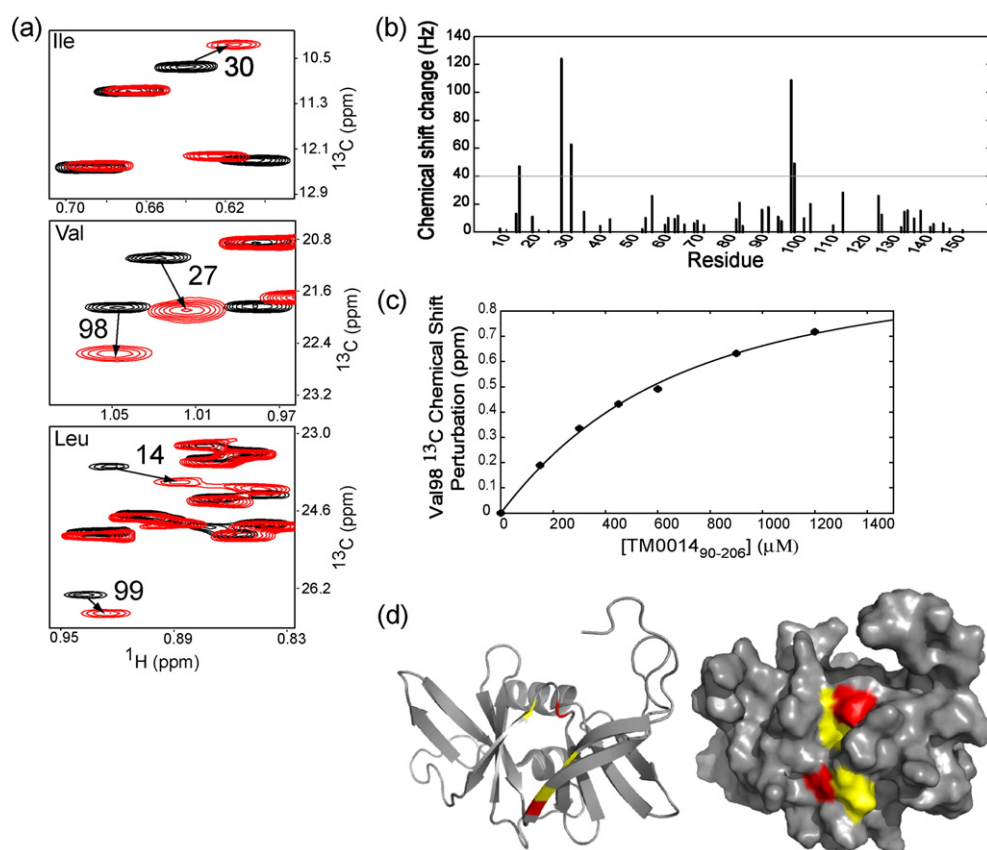


**Fig. 3.** The interaction between the coupling protein CheW and the soluble receptor fragment TM0014<sub>90-206</sub>. (a) A superimposition of  $^1\text{H}$ - $^{13}\text{C}$  HMQC spectra of ILV methyl groups of CheW (black) and CheW in the presence of TM0014<sub>90-206</sub> (red). Residues with significant chemical shifts are numbered with the arrows indicating the direction of the shift. (b) Measured chemical shift perturbations of CheW by the presence of receptor as a function of residue number represented as combined chemical shift  $(\Delta H^2 + \Delta N^2)^{1/2}$  in hertz. (c) Changes in chemical shift of V98 of CheW by TM0014<sub>90-206</sub>. The calculated binding curve is shown with a best-fit dissociation constant of 300 μM. (d) TM0014<sub>90-206</sub> binds to a hydrophobic surface of CheW, formed by  $\beta$ -strands 1, 2, 3, and 8 and the loop bridging  $\beta$ -strands 2 and 3. The residues showing the largest chemical shift changes are shown in red (residues 27 and 98), and the residues with moderate shifts are shown in yellow (residues 14, 30, and 99).

presence of TM0014<sub>90-206</sub> (red), respectively, we observed residue specific chemical shift changes in CheW upon binding TM0014<sub>90-206</sub>. Essentially identical chemical shift changes were observed when we added an excess of intact TM0014 to the methyl-labeled CheW (Supplemental Data S1), showing that the shorter receptor construct contains the same binding site for CheW as the intact receptor. The methyl resonances of CheW residues Val27 and Val98 broadened greatly when bound to protonated TM0014<sub>90-206</sub> but were sharper and could be observed at higher saturation with deuterated receptor. This difference in broadening between using the protonated and deuterated versions of TM0014<sub>90-206</sub> most likely reflects the proximity of the valine methyl groups of CheW to protons on the receptor.<sup>13</sup> The strongly distance dependent dipolar broadening is reduced when the protons of the receptor are replaced by deuterons.

Resonances from other neighboring residues, including Leu14, Ile30, and Leu99, also shifted moderately in the presence of TM0014<sub>90-206</sub>. The largest chemical shift changes were localized in one hydrophobic patch on CheW, as illustrated in the surface representation of CheW shown in Fig. 3d. The residues of CheW with the largest shifts and the residues with more moderate shifts were colored red and yellow, respectively. As can be seen, significant changes in chemical shift were observed in residues located in  $\beta$ -strands 1–3 and 8 of CheW. We assayed the binding affinity of CheW in the presence of TM0014<sub>90-206</sub> by plotting the chemical shift perturbation of a given resonance from its free position by different concentrations of TM0014<sub>90-206</sub>. Several peaks shifted progressively as the receptor fragment was added, showing that the binding was in the fast exchange regime. The titration curve for Val98 was shown in Fig. 3c as a plot of the observed chemical



shift of the methyl resonance of Val98 as a function of TM0014<sub>90–206</sub> concentration. These data were fitted to a hyperbolic binding isotherm, and the dissociation constant was determined to be  $\sim 300$   $\mu\text{M}$ .

#### The CheW binding interface of TM0014<sub>90–206</sub>

The binding surface of TM0014<sub>90–206</sub> in contact with CheW was observed, using a series of  $^1\text{H}$ – $^{15}\text{N}$  TROSY–HSQC spectra of TM0014<sub>90–206</sub> taken over the course of a titration with CheW. Figure 4a showed the superimposition of two  $^1\text{H}$ – $^{15}\text{N}$  HSQC spectra of TM0014<sub>90–206</sub> (black) and the TM0014<sub>90–206</sub>–CheW complex (red). Significant chemical shift changes were observed in TM0014<sub>90–206</sub> due to the binding of CheW. The backbone amide resonances of residues 132, 137, 139, 140, 141, 142, 143, 145, 146, and 156 of TM0014<sub>90–206</sub> shifted significantly when associated with CheW. It should be noted that the

backbone amide of residue 135 did not shift significantly, but its methyl resonance did shift (data not shown). Figure 4b showed the observed chemical shift perturbation for each assigned residue of TM0014<sub>90–206</sub> as a plot of the observed chemical shift change as a function of residue number. Significant chemical shift changes were localized in one area of TM0014<sub>90–206</sub>. Figure 4d showed the residues, with observed combined chemical shift changes above 30 Hz, colored red on the crystal structure of TM0014. These residues formed a well-defined hydrophobic patch at the tip region of TM0014 and were exposed to the solvent where CheW can interact. We estimated the strength of the CheW–receptor interaction by plotting the observed chemical shift of the methyl resonance peak of Ile135 as a function of CheW concentration in Fig. 4c. The curve suggested a dissociation constant of  $\sim 1.2$  mM.

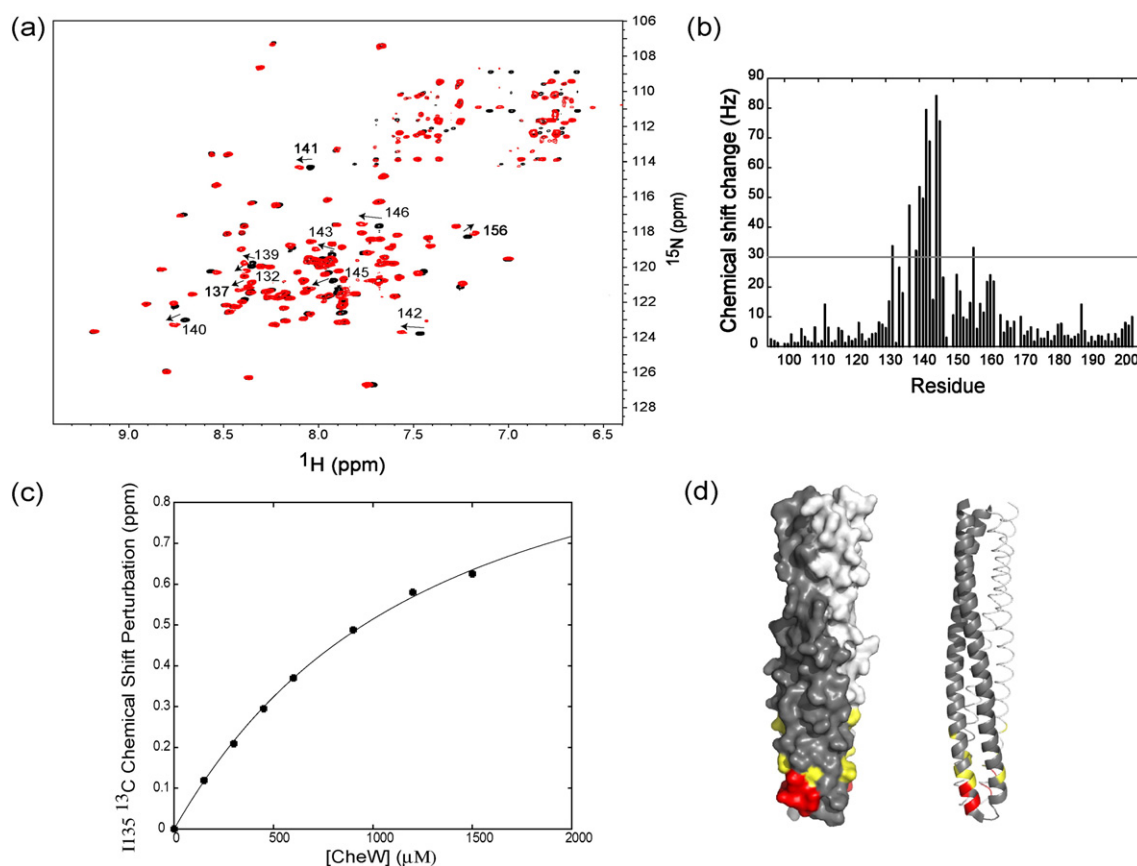


**Fig. 4.** The interaction of TM0014<sub>90–206</sub> with the coupling protein CheW. (a) A superimposition of  $^1\text{H}$ – $^{15}\text{N}$  TROSY–HSQC spectra of TM0014<sub>90–206</sub> (black) and TM0014<sub>90–206</sub> in the presence of CheW (red). Large chemical shift changes (indicated by arrows) are seen in the tip region of the receptor (residues 132, 137, 139, 140, 141, 142, 143, 145, 146, and 156). (b) Measured combined chemical shifts changes in the presence of CheW plotted as a function of residue number for TM0014<sub>90–206</sub>. (c) Changes in chemical shift of TM0014<sub>90–206</sub> as a function of CheW concentration. The calculated binding curve is shown for residue 135 with a best-fit dissociation constant of 1200  $\mu\text{M}$ . (d) Mapping of the residues of TM0014<sub>90–206</sub> perturbed upon binding of CheW on the structure of TM0014<sub>90–206</sub>. Residues with chemical shifts larger than 50 Hz are shown in red; those with shifts between 30 and 50 Hz are shown in yellow.

As shown from the data presented in Fig. 3, the NMR-based titration of labeled CheW by unlabeled receptor fragment suggests an affinity about 4-fold stronger than is observed when labeled receptor is titrated with unlabeled CheW. This discrepancy is well outside of experimental error and reflects the stoichiometry and nature of the CheW–receptor interaction. When CheW is titrated by excess receptor fragment, the binding is predominated by one CheW bound per receptor dimer. However, when receptor fragment is titrated by excess CheW, the binding now reflects a combination of both one and two CheW molecules bound per receptor dimer. If each monomer of the receptor dimer bound CheW identically and independently of whether a CheW was bound at the other monomer, both titrations should show the same apparent affinity. However, if the binding of the first CheW results in a lower affinity for the binding of the second, it would require a higher CheW concentration to fully saturate the receptor dimer than the concentration of receptor needed to saturate CheW. This is exactly what is observed.

## Discussion

Our results suggest that TM0014<sub>90–206</sub> retains the native structure of intact TM0014. Static light-scattering data (data not shown) confirm the dimer nature of the shortened version of TM0014 as expected. The chemical shift index results demonstrate that the secondary structure of TM0014<sub>90–206</sub> consists of two helices with a distinct break at residues 146–151, in agreement with the crystal structure of TM0014. When we superimpose the isoleucine methyl side-chain spectrum of TM0014 with TM0014<sub>90–206</sub> (Supplemental Data S2), TM0014<sub>90–206</sub> shows a subset of the resonances observed for TM0014. This suggests that TM0014 and TM0014<sub>90–206</sub> share a common structure. The TM0014 construct was shortened further to form TM0014<sub>107–191</sub>. TM0014<sub>107–191</sub> has a very different isoleucine methyl chemical shift spectrum when compared to the other two fragments (Supplemental Data S2). In addition, TM0014<sub>107–191</sub> is not as stable as TM0014<sub>90–206</sub> and TM0014, and TM0014<sub>107–191</sub> tends to precipitate at high concentration. This suggests that the length of the receptor plays an important role in maintaining the conformation of the tip region as well as providing structural stability.

In this study, we have identified the interaction interfaces of TM0014<sub>90–206</sub> and CheW complex in solution by chemical shift perturbation techniques. The receptor interaction surface of CheW consists of residues located in the solvent-exposed patches of  $\beta$  strands 1, 3, and 8 as summarized in Fig. 3d. The presence of TM0014 or TM0014<sub>90–206</sub> causes similar

methyl chemical shift changes in the heteronuclear multiple quantum coherence (HMQC) spectra of CheW (see Supplemental Data). This confirms that the binding of TM0014<sub>90–206</sub> and CheW has not been affected by shortening the TM0014 fragment. Previous studies from genetic suppressor screens<sup>7,8</sup> and biochemical assays<sup>5,6</sup> suggested residues of *E. coli* CheW to be important for interaction with the receptors. These homologous residues are also involved in the interaction between CheW and receptor in *T. maritima*, consistent with the high degree of structural similarity, although their amino acid sequences were not very similar.<sup>3,14</sup>

The CheW interaction surface of TM0014<sub>90–206</sub> has been identified and consists mainly of residues near or at the tip region, on the N-terminal side of the tip of the receptor (N-terminal helix). A few residues near the hairpin loop on the C-terminal side (C-terminal helix) of the receptor showed small chemical shift changes when CheW was added. This suggests that the residues on the N-terminal side play a major role, whereas the residues on the C-terminal side play a more minor role in the receptor and CheW interaction. Lui and Parkinson determined a few suppressor mutation sites on the receptors, including two residues located near our proposed binding sites.<sup>7</sup> Mehan *et al.* used chemical modifications to map regions of the *E. coli* receptor Tar that interfered with normal regulation of CheA and found a subpopulation of sites near the receptor tip that inhibited activation of CheA in the presence of CheW.<sup>9</sup> These are in similar locations to those we have identified in TM0014<sub>90–206</sub>. A recent study by Mowery *et al.* showed that all R366 mutants of Tsr, which are equivalent to R146 of TM0014<sub>90–206</sub>, either impaired or destroyed Tsr function, possibly by disrupting the interaction of the receptor and CheW and in turn prevented the formation of the signaling complexes.<sup>15</sup> This evidence seems to agree well with the chemical shift perturbation studies.

Currently, there are two predominant structural models for receptor–receptor interaction in an extended signaling network: the trimer-of-dimers model, based on crystal packing of the *E. coli* serine receptor cytoplasmic domain,<sup>16</sup> and the hedge-row-of-dimers model, based on the crystal packing of a *T. maritima* receptor cytoplasmic domain.<sup>4</sup> The trimer-of-dimers model has been generally supported by electron tomography,<sup>17,18</sup> genetic studies,<sup>19</sup> and biochemical analysis.<sup>20–22</sup> Recently, there has been a report about the universal architecture of chemoreceptor array among many bacteria, including *T. maritima*,<sup>18</sup> that favors the hexagonal symmetry, the trimers of dimers model. In addition, a series of recent studies from the Hazelbauer laboratory suggests that trimers of receptor dimers are critical for receptor function<sup>23–25</sup> in the *E. coli* system. The preponderance of current evidence supports the trimer-of-dimers view of receptor organization.

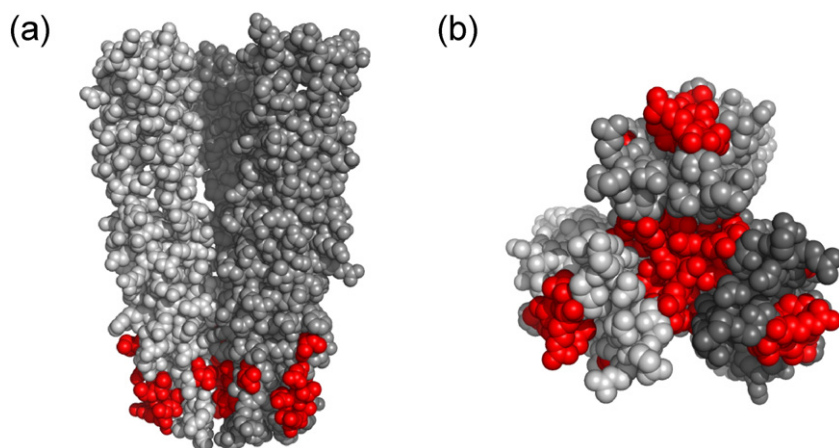


**Fig. 5.** Mapping of contact residues of TM0014<sub>90–206</sub> that are involved in the CheW interaction (red) onto the 3D crystal structure of *E. coli* trimer-of-dimer Tsr receptor. (a) Space-filling side view of cytoplasmic domain of Tsr residues 335–446 in the trimer-of-dimer arrangement. Residues 377, 381, 384, 385, 388, and 398 of Tsr correspond to residues 135, 139, 142, 143, 146, and 156 of TM0014. (b) A bottom view of the space-filling model of the trimer of dimers.

Analysis from the Parkinson laboratory<sup>19</sup> suggests that there are 11 principal trimer contact residues that are highly conserved among chemotactic bacteria. Somewhat surprisingly, 6 of those 11 trimer contact residues are also involved in the receptor and CheW interaction based on our NMR results. These residues were mapped onto the 3D structure of the cytoplasmic domain of Tsr in the trimer-of-dimer arrangement. In Fig. 5, one can see that these residues are also involved in the receptor interaction. This implies that the trimer interface shares similar contact regions with the receptor and CheW. Earlier evidence by Studdert and Parkinson supported this idea. They demonstrated that the presence of CheW and CheA prevented the exchange between members with recently made receptor molecules and stabilized the trimer formation.<sup>21</sup> One explanation could be that the principal trimer contact is blocked by CheW binding to receptors and the formation of trimers of dimers and the interaction between the receptor and CheW are a competitive process. Recently, Cardozo *et al.* showed that over-expression of CheW in *E. coli* cells resulted in disruption of receptor arrays,<sup>26</sup> supporting the notion that CheW binding and trimer formation are competitive processes.

The remarkable sequence conservation observed at the tip of chemotaxis receptors in virtually all motile bacteria is not seen in CheW. CheW homologs show multiple substitutions throughout the sequence, although these changes are generally conservative. This suggests that the receptor tips have a more complex biochemical role, involving receptor array assembly as well as simple binding interactions with CheW and CheA. Previous studies have revealed that most mutants at the tip of the *E. coli* serine receptor are defective in their ability to mediate chemotactic responses, but it has not been easy to assign one simple biochemical defect to these mutations.<sup>19</sup>

The apparent negative cooperativity we observe in CheW binding suggests that there might be steric hindrance caused by CheW binding to the first

binding site of the receptor, which makes it difficult to fit another CheW on the second binding site of the receptor at the relatively small receptor tip. It is also possible that when the first CheW binds, it might produce structural changes in the second binding site that result in lowered affinity. Alternatively, since the P5 domain of CheA is structurally homologous to CheW,<sup>2,5</sup> one of the CheW binding sites on the receptor might be the true binding surface for CheW, while the weaker binding we see could represent the binding surface for the CheA P5 domain on the receptor. The relatively low affinity of the first binding is in contrast to that seen in the *E. coli* system, where CheW appears to bind much more strongly to the chemotaxis receptors.<sup>27</sup> This affinity difference is reversed when considering the CheW–CheA interaction. *Thermotoga* CheW binds much more strongly to its CheA than does the *E. coli* CheW to its CheA. It remains unclear what the physiological consequences might be of these differences in affinity and what role the apparent negative cooperativity we observe may have on the signaling properties of the receptor–CheA–CheW complex.

## Experimental Procedures

### Protein expression and purification

#### Sample preparation

The TM0014 construct was received from Brian Crane's laboratory. PCR methods were used to generate a DNA fragment encoding TM0014 from Lys90 to Thr206 to create a TM0014<sub>90–206</sub> construct. The DNA encoding TM0014<sub>90–206</sub> was subcloned into the vector pET28a (Novagen), and the N-terminal histidine of the His tag was mutated to tyrosine using QuickChange mutagenesis (Stratagene). TM0014<sub>90–206</sub> proteins with an N-terminal His<sub>5</sub> tags were transformed and over-expressed in *E. coli* strain BL21(RIL DE3) (Novagen). During the log phase of bacterial



growth, IPTG was added at 1 mM concentration. U-[ $^{15}\text{N}$ ,  $^{13}\text{C}$ ,  $^2\text{H}$ ]TM0014<sub>90–206</sub> were grown in minimal media, which consisted of 1 mM magnesium sulfate, 0.1 mM calcium chloride, 0.5  $\mu\text{g}/\text{ml}$  of thiamine, and 100  $\mu\text{g}/\text{ml}$  of ampicillin, with the addition of 1 g/l of  $^{15}\text{NH}_4\text{Cl}$  as the main nitrogen source and 2 g/l U-[ $^{13}\text{C}$ ,  $^2\text{H}$ ]glucose or 2 g/l of U-[ $^{12}\text{C}$ ,  $^2\text{H}$ ]glucose (Cambridge Isotope Laboratories, Inc., Andover, MA) as the main carbon source. {[U- $^2\text{H}$ ,  $^{12}\text{C}$ ], Ile $_{\gamma 1}$ -[ $^{13}\text{CH}_3$ ]}TM0014<sub>90–206</sub> and TM0014 and {[U- $^2\text{H}$ ,  $^{12}\text{C}$ ], Ile $_{\gamma 1}$ -[ $^{13}\text{CH}_3$ ], Leu,Val $_{\delta}$ -[ $^{13}\text{CH}_3$ ]}CheW were prepared using the method previously described by Kay laboratory.<sup>12</sup> His<sub>5</sub>-tagged TM0014<sub>90–206</sub> was purified using nickel affinity column (Ni-NTA Agarose; QIAGEN) and size-exclusion chromatography. CheW was over-expressed and purified as previously described.<sup>3</sup> Purified proteins were dialyzed in 50 mM  $\text{Na}_2\text{HPO}_4$  and 1 mM ethylenediaminetetraacetic acid at pH 7.4. All NMR samples contained 0.02% sodium azide and 10%  $\text{D}_2\text{O}$ .

### NMR data collection and processing

NMR data were collected at 40 °C on a Varian 600-Mhz or a Bruker 800-Mhz spectrometer, each using a  $^1\text{H}/^{13}\text{C}/^{15}\text{N}/^2\text{H}$  cryogenically cooled probe equipped with a Z pulsed-field gradient. Sequential assignments of TM0014<sub>90–206</sub> were accomplished with a U-[ $^{15}\text{N}$ ,  $^{13}\text{C}$ ,  $^2\text{H}$ ]sample of TM0014<sub>90–206</sub>, using TROSY-based two-dimensional HSQC and TROSY-based 3D triple-resonance HNCACB,<sup>28–30</sup> HN(CO)CACB, HNCA,<sup>28–33</sup> and HN(CO)CA experiments.<sup>34</sup> All titration experiments were performed. In the first titration, 300  $\mu\text{M}$  {[U- $^2\text{H}$ ,  $^{12}\text{C}$ ], Ile $_{\gamma 1}$ -[ $^{13}\text{CH}_3$ ]}TM0014<sub>90–206</sub> was titrated with  $^2\text{H}$ -labeled CheW to a concentration between 0 and 1500  $\mu\text{M}$ . At each titration point, an HMQC spectrum was collected at 40 °C. The same titration was repeated with 300  $\mu\text{M}$  {[U- $^2\text{H}$ ,  $^{12}\text{C}$ ], Ile $_{\gamma 1}$ -[ $^{13}\text{CH}_3$ ], Leu,Val $_{\delta}$ -[ $^{13}\text{CH}_3$ ]}CheW mixed with varying concentrations of [U- $^2\text{H}$ ]TM0014<sub>107–191</sub> between 0 and 1500  $\mu\text{M}$ . The titration analysis was done assuming fast exchange using 1:1 binding of CheW to TM0014<sub>90–206</sub> monomer units to form the CheW–TM0014<sub>90–206</sub> complex.  $^1\text{H}$ – $^{13}\text{C}$  HMQC spectra were collected at CheW–TM0014<sub>90–206</sub> molar ratios of 0, 0.50, 0.75, 1.0, 2.0, 3.0, 4.0, and 5.0 when methyl TM0014<sub>90–206</sub> spectra were observed. A similar titration was performed to obtain methyl CheW spectra with TM0014<sub>90–206</sub>–CheW molar ratios of 0, 0.50, 0.75, 1.0, 2.0, 3.0, and 4.0. Binding constants were estimated by fitting the observed population-weighted displacement of the resonance peaks from free to bound states during the titration.

### Acknowledgements

We thank Brian Crane and Abiola Pollard (Cornell University) for the TM0014 construct. Robert

Levenson provided discussion and technical advice. This work was support by National Institutes of Health grant GM59544 to F.W.D.

### Supplementary Data

Supplementary data to this article can be found online at [doi:10.1016/j.jmb.2011.11.043](https://doi.org/10.1016/j.jmb.2011.11.043)

### References

1. Hazelbauer, G. L., Falke, J. J. & Parkinson, J. S. (2008). Bacterial chemoreceptors: high-performance signaling in networked arrays. *Trends Biochem. Sci.* **33**, 9–19.
2. Alexander, R. P. & Zhulin, I. B. (2007). Evolutionary genomics reveals conserved structural determinants of signaling and adaptation in microbial chemoreceptors. *Proc. Natl Acad. Sci. USA*, **104**, 2885–2890.
3. Griswold, I. J., Zhou, H., Matison, M., Swanson, R. V., McIntosh, L. P., Simon, M. I. & Dahlquist, F. W. (2002). The solution structure and interactions of CheW from *Thermotoga maritima*. *Nat. Struct. Biol.* **9**, 121–125.
4. Park, S. Y., Borbat, P. P., Gonzalez-Bonet, G., Bhatnagar, J., Pollard, A. M., Freed, J. H. *et al.* (2006). Reconstruction of the chemotaxis receptor–kinase assembly. *Nat. Struct. Mol. Biol.* **13**, 400–407.
5. Boukhvalova, M. S., Dahlquist, F. W. & Stewart, R. C. (2002). CheW binding interactions with CheA and Tar. Importance for chemotaxis signaling in *Escherichia coli*. *J. Biol. Chem.* **277**, 22251–22259.
6. Boukhvalova, M., VanBruggen, R. & Stewart, R. C. (2002). CheA kinase and chemoreceptor interaction surfaces on CheW. *J. Biol. Chem.* **277**, 23596–23603.
7. Liu, J. D. & Parkinson, J. S. (1991). Genetic evidence for interaction between the CheW and Tsr proteins during chemoreceptor signaling by *Escherichia coli*. *J. Bacteriol.* **173**, 4941–4951.
8. Liu, J. D. & Parkinson, J. S. (1989). Role of CheW protein in coupling membrane receptors to the intracellular signaling system of bacterial chemotaxis. *Proc. Natl Acad. Sci. USA*, **86**, 8703–8707.
9. Mehan, R. S., White, N. C. & Falke, J. J. (2003). Mapping out regions on the surface of the aspartate receptor that are essential for kinase activation. *Biochemistry*, **42**, 2952–2959.
10. Pollard, A. M., Bilwes, A. M. & Crane, B. R. (2009). The structure of a soluble chemoreceptor suggests a mechanism for propagating conformational signals. *Biochemistry*, **48**, 1936–1944.
11. Wishart, D. S., Sykes, B. D. & Richards, F. M. (1992). The chemical shift index: a fast and simple method for the assignment of protein secondary structure through NMR spectroscopy. *Biochemistry*, **31**, 1647–1651.
12. Tugarinov, V. & Kay, L. E. (2004). An isotope labeling strategy for methyl TROSY spectroscopy. *J. Biomol. NMR*, **28**, 165–172.
13. Hamel, D. J. & Dahlquist, F. W. (2005). The contact interface of a 120 kD CheA–CheW complex by methyl TROSY interaction spectroscopy. *J. Am. Chem. Soc.* **127**, 9676–9677.



14. Li, Y., Hu, Y., Fu, W., Xia, B. & Jin, C. (2007). Solution structure of the bacterial chemotaxis adaptor protein CheW from *Escherichia coli*. *Biochem. Biophys. Res. Commun.* **360**, 863–867.
15. Mowery, P., Ostler, J. B. & Parkinson, J. S. (2008). Different signaling roles of two conserved residues in the cytoplasmic hairpin tip of Tsr, the *Escherichia coli* serine chemoreceptor. *J. Bacteriol.* **190**, 8065–8074.
16. Kim, K. K., Yokota, H. & Kim, S. H. (1999). Four-helical-bundle structure of the cytoplasmic domain of a serine chemotaxis receptor. *Nature*, **400**, 787–792.
17. Zhang, P., Khursigara, C. M., Hartnell, L. M. & Subramaniam, S. (2007). Direct visualization of *Escherichia coli* chemotaxis receptor arrays using cryo-electron microscopy. *Proc. Natl Acad. Sci. USA*, **104**, 3777–3781.
18. Briegel, A., Ortega, D. R., Tocheva, E. I., Wuichet, K., Li, Z., Chen, S. *et al.* (2009). Universal architecture of bacterial chemoreceptor arrays. *Proc. Natl Acad. Sci. USA*, **106**, 17181–17186.
19. Ames, P., Studdert, C. A., Reiser, R. H. & Parkinson, J. S. (2002). Collaborative signaling by mixed chemoreceptor teams in *Escherichia coli*. *Proc. Natl Acad. Sci. USA*, **99**, 7060–7065.
20. Studdert, C. A. & Parkinson, J. S. (2005). Insights into the organization and dynamics of bacterial chemoreceptor clusters through *in vivo* crosslinking studies. *Proc. Natl Acad. Sci. USA*, **102**, 15623–15628.
21. Studdert, C. A. & Parkinson, J. S. (2004). Crosslinking snapshots of bacterial chemoreceptor squads. *Proc. Natl Acad. Sci. USA*, **101**, 2117–2122.
22. Parkinson, J. S., Ames, P. & Studdert, C. A. (2005). Collaborative signaling by bacterial chemoreceptors. *Curr. Opin. Microbiol.* **8**, 116–121.
23. Li, M. & Hazelbauer, G. L. (2011). Core unit of chemotaxis signaling complexes. *Proc. Natl Acad. Sci. USA*, **108**, 9390–9395.
24. Li, M., Khursigara, C. M., Subramaniam, S. & Hazelbauer, G. L. (2011). Chemotaxis kinase CheA is activated by three neighbouring chemoreceptor dimers as effectively as by receptor clusters. *Mol. Microbiol.* **79**, 677–685.
25. Boldog, T., Li, M. & Hazelbauer, G. L. (2007). Using Nanodiscs to create water-soluble transmembrane chemoreceptors inserted in lipid bilayers. *Method Enzymol.* **423**, 317–335.
26. Cardozo, M. J., Massazza, D. A., Parkinson, J. S. & Studdert, C. A. (2010). Disruption of chemoreceptor signalling arrays by high levels of CheW, the receptor–kinase coupling protein. *Mol. Microbiol.* **75**, 1171–1181.
27. Gegner, J. A., Graham, D. R., Roth, A. F. & Dahlquist, F. W. (1992). Assembly of an MCP receptor, CheW, and kinase CheA complex in the bacterial chemotaxis signal transduction pathway. *Cell*, **70**, 975–982.
28. Salzmann, M., Pervushin, K., Wider, G., Senn, H. & Wuthrich, K. (1999). [<sup>13</sup>C]-constant-time [<sup>15</sup>N, <sup>1</sup>H]-TROSY-HNCA for sequential assignments of large proteins. *J. Biomol. NMR*, **14**, 85–88.
29. Loria, J. P., Rance, M. & Palmer, A. G., III (1999). Transverse-relaxation-optimized (TROSY) gradient-enhanced triple-resonance NMR spectroscopy. *J. Magn. Reson.* **141**, 180–184.
30. Meissner, A. & Sorensen, O. W. (2001). Sequential HNCACB and CBCANH protein NMR pulse sequences. *J. Magn. Reson.* **151**, 328–331.
31. Salzmann, M., Pervushin, K., Wider, G., Senn, H. & Wuthrich, K. (1998). TROSY in triple-resonance experiments: new perspectives for sequential NMR assignment of large proteins. *Proc. Natl Acad. Sci. USA*, **95**, 13585–13590.
32. Pervushin, K., Gallius, V. & Ritter, C. (2001). Improved TROSY-HNCA experiment with suppression of conformational exchange induced relaxation. *J. Biomol. NMR*, **21**, 161–166.
33. Salzmann, M., Wider, G., Pervushin, K. & Wuthrich, K. (1999). Improved sensitivity and coherence selection for [<sup>15</sup>N, <sup>1</sup>H]-TROSY elements in triple resonance experiments. *J. Biomol. NMR*, **15**, 181–184.
34. Yang, D. & Kay, L. E. (1999). Improved lineshape and sensitivity in the HNCO-family of triple resonance experiments. *J. Biomol. NMR*, **14**, 273–276.